ASSIMILATION OF TOMOGRAPHIC PARTICLE IMAGE VELOCIMETRY DATA OF TURBULENT MIXED CONVECTION IN A CUBOIDAL CELL

Christian Bauer[a,*], **Michael Mommert**[a] **and Claus Wagner**[a,b]
[a]Institute of Aerodynamics and Flow Technology
German Aerospace Center, Göttingen, Germany
[b]Institute of Thermodynamics and Fluid Mechanics
Technische Universität Ilmenau, Germany

*christian.bauer@dlr.de

Keywords: tomographic particle image velocimetry, turbulent mixed convection, data assimilation, direct numerical simulation

1. INTRODUCTION

Data assimilation, i.e. applying numerical algorithms on experimental data to extract additional information, has become an increasingly important topic in the field of fluid dynamics and turbulence research in the past decades (di Leoni et al. 2020). Although tomographic particle image velocimetry (tomo PIV) allows to capture largely temporally and spatially resolved, three-dimensional velocity fields of turbulent flow, usually not all essential parts of the flow problem can be measured. Due to the reflection of the laser light sheet and low tracer particle densities near solid walls, boundary layers are often difficult to capture using PIV. In addition, turbulent small-scale structures are often filtered out, since velocity vectors represent surface- or volume-averaged quantities obtained from a correlation step.

Moreover, for fluid problems involving thermal convection, the temperature field—next to the velocity field—is essential for the flow problem. However, to capture the temperature field simultaneously with the velocity field requires additional elaborate measurement techniques which are often not feasible.

Thus, Bauer et al. (2022) present an algorithm for the problem of turbulent Rayleigh–Bénard convection that allows to assimilate tomo PIV measured velocity fields and extract corresponding temperature fields without additional measurements, but solely by exploiting the governing flow equations. In our present work, we extend our data assimilation scheme to the problem of turbulent mixed convection in a cuboidal cell, where pressure-driven forces act on the flow besides buoyancy. Moreover, we use the assimilation scheme to expand the measurement data from one fourth of the complete sample of Mommert et al. (2020) to the entire sample, i.e. to regions that were not initially captured by the tomo PIV measurements (see Figure 1).

The extended abstract is organized as follows: In Section 2, the experimental set up of the mixed convection cell measurement is introduced. Subsequently, the data assimilation algorithm applied to the measured velocity field as well as the first results are depicted in section 3. Finally, the abstract is concluded in section 4.

2. EXPERIMENTAL SET UP

The experimental data set is obtained from the tomographic PIV (tomo PIV, Elsinga, 2006) measurement of a mixed convection cell reported by Mommert et al. (2020). The experiment consists of a rectangular sample with dimensions L_x=2500mm, L_y=L_z= $\widehat{H}$ =500mm, as shown in Figure 1.

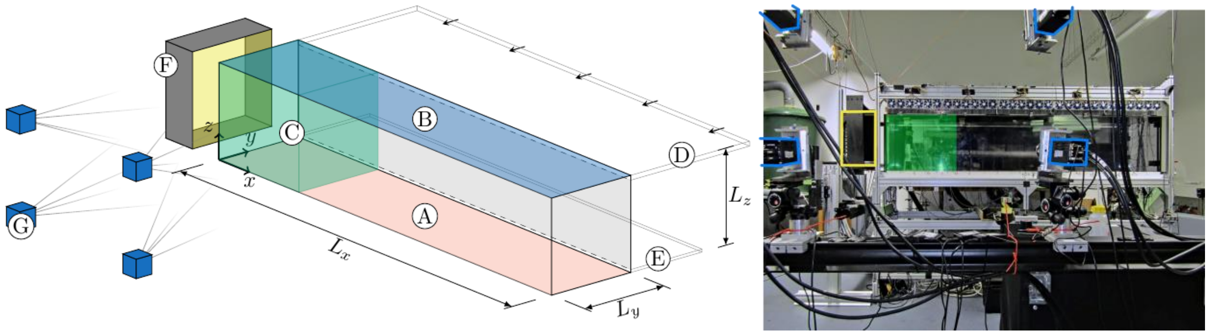

Figure 1. Left: Sketch of the mixed convection sample with heated bottom (A) and cooled top plate (B); Measurement volume (C); Velocity inlet (D) and outlet (E); LED light system (F) and PIV camera system (G). Right: Photograph of the mixed convection sample. Figure adapted from Mommert et al. (2020).

The aluminum bottom plate (A) is heated by tempered water whereas the aluminum top plate (B) is passively cooled to room temperature. In order to minimise heat exchange with the surroundings while allowing optical access, the side walls of the sample were made of double-walled, 10mm-thick polycarbonate. Moreover, a 25mm high velocity inlet (D) and a 15mm high velocity outlet (E) were attached to the top and the bottom edge, respectively. The flow in a subvolume of the mixed convection cell (C) is captured by tracking helium-filled soap bubbles illuminated by an LED light system (F) with a PIV camera system (G). For more details the reader is referred to Mommert et al. (2020).

3. DATA ASSIMILATION SCHEME

The flow of turbulent mixed convection can be characterised by the Prandtl number $\mathrm{Pr} = \hat{\nu}/\hat{\kappa}$, representing the ratio of momentum diffusivity and thermal diffusivity, the Rayleigh number $\mathrm{Ra} = \hat{\alpha}\hat{g}\hat{H}\Delta\hat{T}/(\hat{\nu}\hat{\kappa})$, reflecting the ratio of buoyancy and diffusive forces, and the Reynolds number $\mathrm{Re} = \hat{u}_{in}\hat{H}/\hat{\nu}$, representing the ratio of inertial and viscous forces, with $\hat{\nu}$ the kinematic viscosity, $\hat{\kappa}$ the thermal diffusivity, $\hat{\alpha}$ the thermal expansion coefficient, $\hat{g}$ the gravitational acceleration, $\hat{H}$ the mixed convection cell height, $\Delta\hat{T}$ the vertical temperature difference, and $\hat{u}_{in}$ the inlet velocity. In the following, dimensional quantities are denoted with circumflex and the dimensionless without. The equations governing the problem are the transport equations for mass, momentum, and energy, which for an incompressible fluid and the Boussinesq approximation read in dimensionless form

$$\nabla \cdot \boldsymbol{u} \;=\; \mathbf{0}, \tag{1}$$

$$\frac{\partial \mathbf{u}}{\partial t} + \boldsymbol{u} \cdot \nabla \boldsymbol{u} = -\nabla p + \sqrt{\frac{\mathrm{Pr}}{\mathrm{Ra}}}\nabla^2 \boldsymbol{u} + T\boldsymbol{e_z}, \tag{2}$$

$$\frac{\partial T}{\partial t} + \boldsymbol{u} \cdot \nabla T = \sqrt{\frac{1}{\mathrm{PrRa}}}\nabla^2 T, \tag{3}$$

with $\mathbf{u}$ the velocity vector (u_x,u_y,u_z), p the pressure, T the temperature and $\mathbf{e_z}$ the unit vector in vertical direction. In experimentally-measured data, the conservation of mass, equation (1), is often not fulfilled. Hence, we apply the following algorithm to the measured velocity field to ensure the divergence-free condition: First, we compute the divergence of the measured velocity field. Then, a pseudo-pressure is obtained by solving the Poisson equation for the measured velocity field. Finally, the velocity field is corrected via the pseudo-pressure. Figure 2 portrays the vertical velocity component v in an xz-plane at y/h=0.5 before (a) and after the divergence has been removed (b) as well as the divergence of the measured velocity field (c).

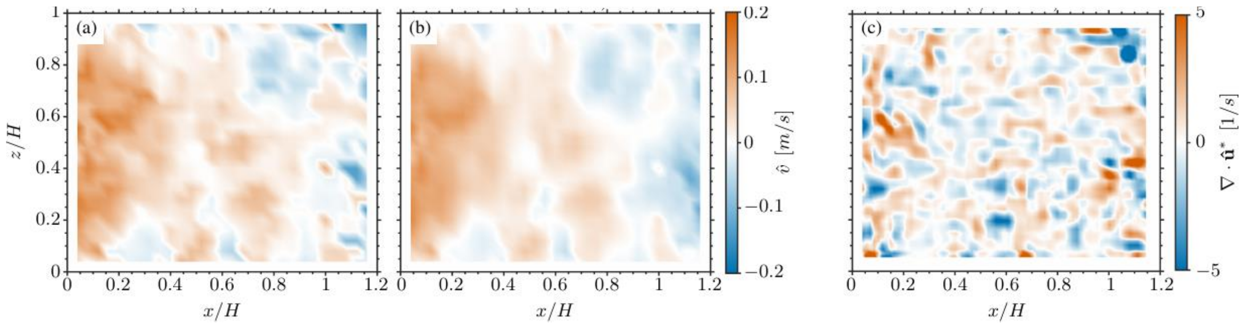

Figure 2. The v velocity component before (a) and after (b) divergence has been removed in an xz-plane at y/h=0.5. (c) The divergence of the initial tomo PIV measured velocity field.

As Figure 2 indicates, our algorithm successfully removes discontinuities from the measured velocity data by imposing the divergence-free condition. The obtained divergence-free velocity fields are then fed into a nudging algorithm, which is a further development of the algorithm we used for Rayleigh–Bénard convection (Bauer et al., 2022) and similar to the one introduced by Suzuki and Yamamto (2015). Starting from an initial velocity and temperature field provided by a direct numerical simulation conducted for the characteristic dimensionless numbers of the experiment Ra=1.4×10^8, Re=7350, and Pr=0.7 for air, the governing equations (1-3) are integrated in time with the momentum equation being expanded by a feedback term that penalizes the deviation of the computed velocity from the experimentally-obtained, divergence-free velocity field, i.e.

$$\frac{\partial \mathbf{u}}{\partial t} + \boldsymbol{u} \cdot \nabla \boldsymbol{u} = -\nabla p + \sqrt{\frac{\mathrm{Pr}}{\mathrm{Ra}}}\nabla^2 \boldsymbol{u} + T\boldsymbol{e_z} + \alpha(\boldsymbol{u_{ref}} - \boldsymbol{u}), \tag{4}$$

where α is the feedback gain and $\boldsymbol{u_{ref}}$ represents the experimentally-obtained, divergence-free velocity field linearly interpolated from two consecutive snapshots. A schematic sketch of the algorithm is depicted in Figure 3 (left). In the subvolume of the mixed convection sample where tomo PIV velocity data has been captured (green volume in Figure 1), the time-integrated velocity field is every time step subjected to a force, which is proportional to the deviation of the velocity field from the corresponding tomo PIV velocity field. Thus, after an initial transient phase, the simulated flow field evolves towards the measured one in the measurement volume, while its extension in the rest of the sample evolves accordingly due to the conservation of mass, momentum and energy (equations 1-3). As a consequence, the flow field becomes accessible not only in the measurement volume, but also in the rest of the sample as well as in the boundary layers in the vicinity of solid walls, which have not been captured, initially. Furthermore, the temperature field that corresponds to the simulated velocity field, and therefore, to the measured velocity field, becomes accessible as well. As a preliminary result, Figure 3 (right) displays the measured velocity field together with the corresponding simulated velocity and temperature fields during the initial transient phase.

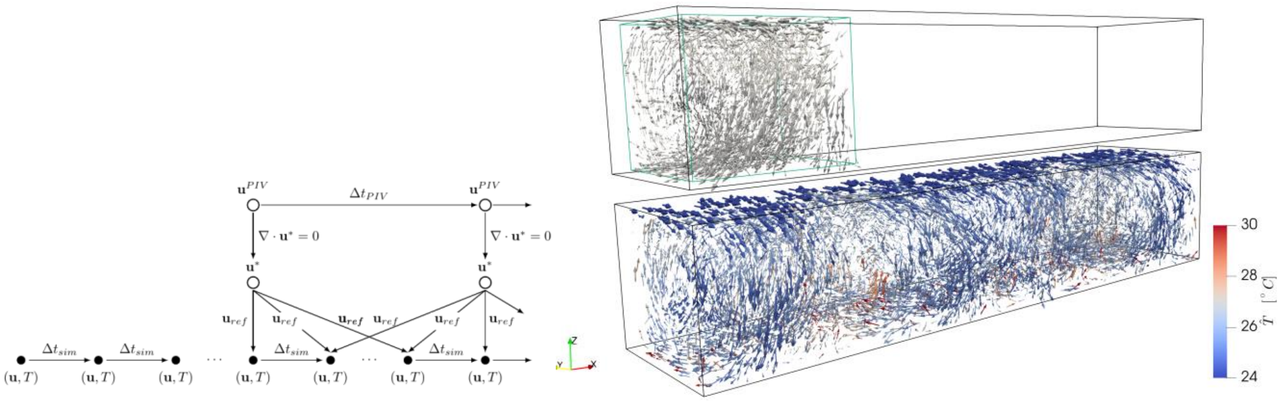

Figure 3. Left: Schematic sketch of the nudging algorithm. $\mathbf{u}$, time-integrated velocity; T, time-integrated temperature; $\mathbf{u}^{\mathrm{PIV}}$, tomo PIV-measured velocity; $\mathbf{u}^*$, divergence-free velocity for each tomo PIV snapshot; $\mathbf{u}_{\mathrm{ref}}$, linearly interpolated velocity at every time step from consecutive PIV snapshots; Δt_{sim}, simulation time step; Δt_{PIV}, tomo PIV time step. Right: Measured tomo PIV velocity field $\mathbf{u}^{\mathrm{PIV}}$ (top) and preliminary simulated velocity and temperature fields $\mathbf{u}$, T (bottom).

4. CONCLUSIONS

In order to extract additional information from tomo PIV measured velocity fields of turbulent mixed convection as well as to extend the measurement domain, we adapt our recently published data assimilation scheme (Bauer et al., 2022), considering the governing equations of the problem. The divergence-free condition is fulfilled by solving the Poisson equation for the experimentally-measured velocity field and by correcting the fields according to a fractional step method (see Figure 2). Moreover, since the measurement contains only data of approximately one-fourth of the flow domain, we are expanding the measured velocity field to the flow region where no data has been measured by applying the nudging algorithm sketched in Bauer et al (2022). In this way, we do not only increase the quality of the velocity measurement by making it divergence-free, but we also assess parameters that are not directly measured—such as the pressure and the temperature—and expand them into regions that have not been accessible by the measurement, as well. At the conference, we are going to present and evaluate velocity and temperature fields of turbulent mixed convection extracted from tomo PIV measurements with the methods mentioned above. We strongly believe that such methods are a valuable contribution to the field of PIV measurements, as they help to extract information initially hidden in the measurement data without additional measurements.

5. REFERENCES

Bauer, C., Schiepel, D. and Wagner, C., 2022. “Assimilation and extension of particle image velocimetry data of turbulent Rayleigh–Bénard convection using direct numerical simulations”. *Experiments in Fluids*, Vol. 63(22), pp. 1-17.

Di Leoni, P.C., Mazzino, A. and Biferale, L., 2020. “Synchronization to big data: Nudging the Navier-Stokes equations for data assimilation of turbulent flows”. *Physical Review X,* Vol. 10(1), 011023.

Elsinga, G.E., Scarano, F., Wieneke, B. and van Oudheusden, B.W., 2006 “Tomographic particle image velocimetry”. *Experiments in Fluids*, Vol. 41(6), pp. 933-947.

Mommert, M., Schiepel, D., Schmeling, D. and Wagner, C., 2020. “Reversals of coherent structures in turbulent mixed convection”. *Journal of Fluid Mechanics*, Vol. 904, A33.

Schiepel, D., Schmeling, D. and Wagner, C., 2021. “Simultaneous tomographic particle image velocimetry and thermometry of turbulent Rayleigh–Bénard convection”. *Measurement Sciences and Technology*, Vol. 32(9), 095201.

Suzuki, T. and Yamamoto, F., 2015. “Hierarchy of hybrid unsteady flow simulations integrating time-resolved PTV with DNS and their data-assimilation capabilities”. *Fluid Dynamics Research*, Vol 47(5), 051407.